

---

# Research on numerical simulation method of preparation process of highly active photocatalytic nanomaterials

---

Liyin Zhang

School of Materials Science and Engineering,  
Nanyang Technological University, Singapore  
Email: liyinz@mls.sinanet.com

**Abstract:** In order to degrade organic pollutants, a numerical simulation method for the preparation of highly active photocatalytic nanomaterials was proposed. TiO<sub>2</sub> nanomaterial samples were prepared by electrochemical anodisation method, and C-240 TiO<sub>2</sub> nanomaterial powder samples were obtained. The structure of C-240 samples was analysed by X-ray diffraction. Methyl orange and p-chlorophenol were selected as degradation pollutants. The visible light catalytic activity of C-240 TiO<sub>2</sub> nanomaterials was characterised by UV-vis absorption spectrum. According to the UV-vis spectra of C-240 samples and commercial P-25 samples for 60 min of photocatalytic degradation of methyl orange, and the UV-vis spectra of C-240/180 samples for 60 min of photocatalytic degradation of p-chlorophenol under visible light, it was found that C-240 sample had more than 90% photocatalytic degradation of methyl orange, and C-240/180 sample had 66% degradation rate of p-chlorophenol. Compared with commercial P-25, it had higher catalytic degradation performance.

**Keywords:** catalytic degradation; nanomaterials; ray diffraction method; structure characterisation; degradation rate.

**Reference** to this paper should be made as follows: Zhang, L. (2021) 'Research on numerical simulation method of preparation process of highly active photocatalytic nanomaterials', *Int. J. Materials and Product Technology*, Vol. 63, Nos. 1/2, pp.59–71.

**Biographical notes:** Liyin Zhang is a Master's student in School of Materials Science and Engineering of Nanyang Technological University, Singapore. She graduated from the Northwest University with a Bachelor's in Materials Chemistry. She has certain research on electrocatalysis and degradable materials.

---

## 1 Introduction

Science and technology are becoming more and more advanced, and the organic pollutants produced have caused damage to the environment, so research on the degradation of organic pollutants has become the top priority at present. The use of photocatalytic technology to degrade organic pollutants effectively solves the problem of organic pollution in the industry in the fastest time (Shu et al., 2019). Photocatalytic technology is a chemical method with higher practicality and lower cost. It chemically

combines light and catalyst, and eliminates pollutants in the water phase and gas phase, and improves the pollution control rate (Zhang et al., 2018). Nanomaterials are industrial raw materials that are usually used in major industries such as fuels and coatings. Nanomaterials can electrolyse water through electrodes using ultraviolet light, and have been widely used in the field of photocatalysis due to their advantages. Therefore, related research on nanomaterials photocatalytic oxidation technology has attracted the attention of many scholars. The use of nanomaterials photocatalytic oxidation technology for wastewater treatment is one of the most important methods at present. The use of photocatalytic nanomaterials can prepare a photocatalyst, which can be used to perform photocatalysis under ultraviolet light to degrade organic pollutants. To meet the requirements of environmental governance, the photocatalytic nanomaterials are not only environmentally friendly, but also low in cost. They are more commonly used in real life and provide certain help for people's lives and industrial production (Shankar et al., 2018). However, the band gap of nanomaterials is relatively wide, and the wavelength of ultraviolet light can only excite the band gap of nanomaterials within 387 nm, and the ultraviolet light in sunlight has a low occupancy rate, resulting in low utilisation of nanomaterials for sunlight. Therefore, it is difficult to degrade high-concentration organic pollutants using ordinary nanomaterials, which makes it difficult to treat large amounts of high-concentration industrial wastewater. Therefore, the preparation of highly active photocatalytic nanomaterials has a certain effect on the research of photocatalytic technology. With the continuous development of nanoscience, the size of materials is getting smaller and smaller, and there is no specific requirement for the size of the crystal grains in the material. Therefore, the preparation of high-activity photocatalytic nanomaterials is relatively broad in the choice of materials (Zhou et al., 2020).

In recent years, with scholars' in-depth research on numerical simulation methods for the preparation of highly active photocatalytic nanomaterials, more and more fruitful results have been achieved. Li et al. (2018b) is based on the anodic oxidation method and continuous ion layer adsorption method to prepare high catalytic activity composite nanomaterials. The prepared nanomaterials have a narrow band gap and are evenly distributed in the nanonet. The prepared high catalytic activity composite nanomaterials are improved. The absorption rate and degradation rate of visible light. Liu et al. (2019) uses a hydrothermal method to prepare photocatalytic nanomaterials. This method uses X-ray diffraction technology and scanning electron microscopy to obtain ray diffraction patterns and scanning electron microscopy images of nanomaterials, and uses high-temperature pyrolysis to degrade them to obtain nanomaterial samples structure, analyse the difference in the structure morphology and photocatalytic performance of nanomaterials with different doping amounts. Experimental tests show that the doping amount is more average for the nanometer particle size, and the grain size in the nanomaterial is smaller, but at temperature if it is too high, the photocatalytic performance will decrease.

Based on the above research, this paper proposes a numerical simulation method for the preparation of highly active photocatalytic nanomaterials. The research technical route of this method is as follows:

- 1 First, process the substrate used in the experiment, and then configure the electrolyte needed for the experiment. After the preparation is completed, prepare the TiO<sub>2</sub> nanomaterial sample by anodising method, and preprocess the sample.
- 2 Then the structure characterisation of TiO<sub>2</sub> nanomaterials was analysed by ray diffraction method. Finally, the photocatalytic activity test was carried out in the photocatalytic experiment reaction device, and it was found that the material prepared in this paper has high activity of visible light catalytic degradation performance.

## 2 Numerical simulation method for preparation process of highly active photocatalytic nanomaterials

### 2.1 Experimental reagents and equipment

#### 2.1.1 Experimental reagent

The main reagents required for the preparation of highly active photocatalytic TiO<sub>2</sub> nanomaterials are shown in Table 1.

**Table 1** Experimental reagents and manufacturers

<i>Reagent name</i>	<i>Name of manufacturer</i>
Ferric chloride [FeCl <sub>3</sub> ], A.R.	Sinopharm Group
Sodium dihydrogen phosphate [NaH <sub>2</sub> PO <sub>4</sub> ], A.R.	Sinopharm Group
Polyvinylpyrrolidone [PVP, K-30], A.R.	Aldrich
Titanium powder [Ti], A.R.	Sinopharm Group
Hydrogen fluoride [HF], A.R.	Laizhou Kangde Chemical Co., Ltd.
2 thiolactic acid	Sinopharm Group
Copper nitrate [Cu (NO <sub>3</sub> ) <sub>2</sub> 3H <sub>2</sub> O], A.R.	Sinopharm Group
Sodium sulphide [NA <sub>2</sub> S9H <sub>2</sub> O], A.R.	Shanghai Tongya Chemical Technology Co., Ltd.
Tetrabutyl titanate (C <sub>16</sub> H <sub>36</sub> O <sub>4</sub> Ti), C.P.	Sinopharm Group
Toluene (C <sub>7</sub> H <sub>8</sub> ), A.R.	Sinopharm Group
Oleic acid (C <sub>17</sub> H <sub>33</sub> COOH), A.R.	Sinopharm Group
Titanium tetrafluoride [TiF <sub>4</sub> ]	Self-control
Iron oleate [(C <sub>17</sub> H <sub>33</sub> COO) <sub>3</sub> Fe]	Self-control
Deionised water	Self-made water system

#### 2.1.2 Experimental equipment

The main instruments and equipment used in the preparation of highly active photocatalytic TiO<sub>2</sub> nanomaterials are shown in Table 2.

**Table 2** Experimental equipment

<i>Equipment name</i>	<i>Manufacturer</i>
Ultrasonic cleaner	Ultrasonic Instrument Co., Ltd.
Electronic balance	Shanghai Liangping Instrument Co., Ltd.
The pure water purification system of Yupu	Chengdu Chaochun Technology Co., Ltd.
Vacuum drying oven	Beijing Yongguangming Medical Instrument Factory
X-ray diffractometer	Rigaku
Thermal field emission scanning electron microscopy	Hitachi
Photochemical reaction instrument	Nanjing Xujiang Electromechanical Plant
Infrared spectrophotometer	Hitachi
Constant temperature heating magnetic stirrer	Hitachi
Centrifuge	Shanghai Anting Scientific Instrument Factory

### 2.1.3 Substrate processing

Before the preparation of high-activity photocatalytic TiO<sub>2</sub> nanomaterials, the experimental substrate was first processed. Conductive glass and silicon were used as the experimental substrates. Since the substrate would be contaminated, the adhesion of the prepared nanomaterials would decrease, which would affect the material. Therefore, all the substrates used in the experiment are cleaned before preparation to ensure the quality of the materials (Huang et al., 2019; Chen et al., 2018; Hashempour and Vakili, 2018). The processing steps of the substrate are as follows:

- 1 the experimental environment is a sterile environment, and the substrate is simply cleaned for 2/3 h under aseptic conditions to achieve the purpose of clean material and no impurities
- 2 after the substrate is simply cleaned, wipe the clean substrate again with alcohol and place it in a sterile box for two days to ensure that the substrate is not contaminated
- 3 after two days, take out the substrate from the sterile box and rinse again with high-purity water
- 4 after rinsing is complete, dry it for later use.

## 2.2 Experimental method

### 2.2.1 Titanium pretreatment

Cut 10 cm \* 10 cm titanium pieces into 1 cm \* 1.5 cm pieces, drill holes above each piece, and use high-purity water to repeatedly clean the drilled titanium pieces in a sterile environment for 2/3 h, and then dry by natural wind. Use a thin copper wire to pass through the small holes in all the titanium sheets, and use insulating cloth strips to wind all the connected small titanium sheets, leaving a distance of 1 cm between the small holes and the cloth strips.

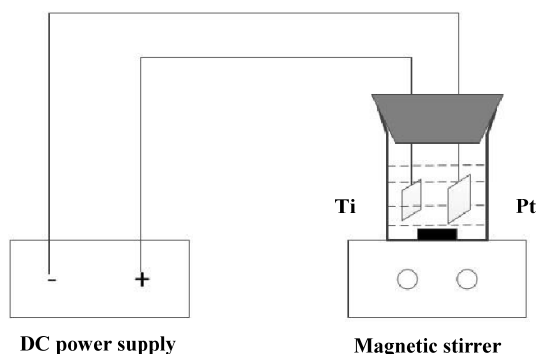
### 2.2.2 Electrolyte preparation

Fuse glycerol and water in different volume ratios, add a small amount of ionic compounds to the mixed solution, and stir evenly with a magnetic stirrer. After the plasma compound is fully dissolved in the mixed solution, the electrolyte preparation is completed (Wang et al., 2020; Zheng et al., 2019; Du et al., 2018).

### 2.2.3 $TiO_2$ nanomaterial sample preparation

In this paper, after the above preparation, through the two electrode system, select the above treated titanium sheet as anode, Pt electrode as cathode, at room temperature and humidity of 50%, through the above prepared electrolyte, using the anodic oxidation method to prepare  $TiO_2$  nanomaterial samples. Figure 1 is the schematic diagram of the preparation device.

**Figure 1** Schematic diagram of the device for preparing  $TiO_2$  nanomaterial samples by electrochemical anodisation



After the preparation, rinse the prepared samples with distilled water and blow dry (Attallah et al., 2020; Zeng et al., 2018; Mao et al., 2019).

### 2.2.4 Pretreatment

In order to improve the effectiveness of experimental research and eliminate the interference of other irrelevant factors, the experimental materials were pretreated. In a dry environment, pretreat the  $TiO_2$  nanomaterial sample prepared by the anodisation method, fuse 60 ml of acetone, 20 ml of pyridine, and 14 ml of ethanol, add 20 ml of butyl titanate to the mixed solution, stir evenly, and mix the pour the mixed solution into the  $\phi = 50$  mm,  $h = 100$  mm reaction tube placed in the WHF-0.25 L high-pressure reactor, pour 1.5 ml of water between the reaction tube and the reactor, and seal it in a  $3^\circ C/min$  incubator (Wu et al., 2018b). As time continues to rise, water vapour will be generated under the reactor, which will slowly flow into the reaction tube, and the water vapour will undergo a hydrolysis reaction with butyl titanate. After cooling, take out a sample of C-240  $TiO_2$  nanomaterial and use Wipe it with alcohol to keep it free of impurities. After wiping, place it in a sterile box for two days, and sample in a sterile box after two days.

### 2.3 Structural characterisation and analysis of TiO<sub>2</sub> nanomaterials

After the pretreatment of the above-mentioned TiO<sub>2</sub> nanomaterial sample, a C-240 TiO<sub>2</sub> nanomaterial powder sample is obtained, and the structure characterisation of the C-240 TiO<sub>2</sub> nanomaterial powder sample is analysed by the ray diffraction method. The ray diffraction method is to hit electrons on the target under accelerating voltage, and shoot the characteristic rays generated by the electrons into the sample, and collide with crystal atoms, so that diffraction intensity peaks of different intensities appear, and the crystal grains are calculated according to the positions of the diffraction peaks size.

Under the accelerating voltage, irradiate the generated radiation on the surface of the C-240 TiO<sub>2</sub> nanomaterial sample, and use the collecting instrument to collect the general line characteristics of the radiation, analyse the structure and composition of the C-240 TiO<sub>2</sub> nanomaterial sample, and obtain the crystal lattice of the sample through computer software parameters (Wu et al., 2018a; Wang, 2019). Using the Bragg equation, at a working voltage of 40 kV and a working current of 250 mA, the geometric relationship between the incident light and the crystal is analysed, and diffraction lines are obtained to calculate the crystal size (Li et al., 2018a; Ilieva et al., 2018).

Calculate the layer spacing  $d_{hkl}$  of the tested sample according to the Bragg equation, the expression is:

$$d_{hkl} = \frac{\lambda}{2 \sin \theta} \quad (1)$$

In the formula,  $\lambda$  represents the ray wavelength and  $\theta$  represents the diffraction angle.

Since the particle size is inversely proportional to the half-height width of the diffraction peak, the crystal grain size  $D$  of the TiO<sub>2</sub> nanomaterial sample can be determined according to the obtained layer spacing:

$$D = \frac{K\lambda d_{hkl}}{B \cos \theta} \quad (2)$$

In the formula,  $K$  represents the diffraction coefficient, and  $B$  represents the half-width of the diffraction peak.

## 3 Results and discussion

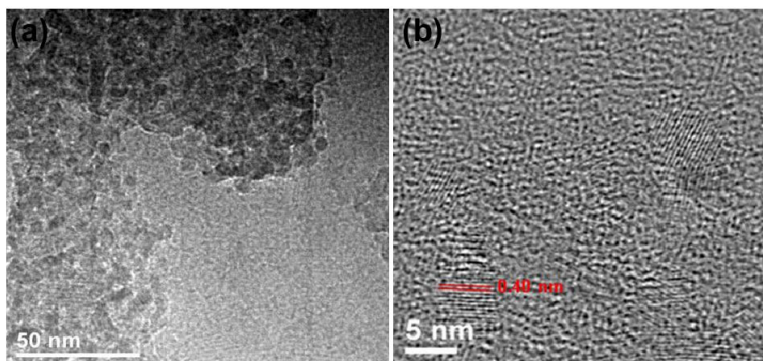
### 3.1 Shape analysis

The C-240 TiO<sub>2</sub> nanomaterial samples prepared by electrochemical anodisation were analysed by transmission electron microscopy and high resolution transmission electron microscopy. Figure 2 shows the TEM and HRTEM images of the C-240 TiO<sub>2</sub> nanomaterial.

From the TEM image of the C-240 TiO<sub>2</sub> nanomaterial in Figure 2(a), it can be seen that the C-240 TiO<sub>2</sub> nanomaterial has a certain degree of agglomeration, but a single spherical particle with a diameter of about 5 nm can still be found. Analysing the HRTEM image in Figure 2(b), it can be seen that the C-240 sample has a very obvious strip-like lattice, and the distance between the lattices is 0.4 nm [shown by the red line in

Figure 2(b)]. What is clear is that its diameter is only 5nm and the surface has titanium atom particles.

**Figure 2** TEM and HRTEM images of C-240 TiO<sub>2</sub> nanomaterial (see online version for colours)



### 3.2 Photocatalytic activity test

The photocatalytic activity of C-240 TiO<sub>2</sub> nanomaterials was tested by degrading azo dye methyl orange and aromatic compound p-chlorophenol, and its characterisation was analysed.

In the absence of light, mix 30 mg of C-240 TiO<sub>2</sub> nanomaterials and 15 mlmg/L of methyl orange solution or p-chlorophenol solution, put the mixed solution in the reactor and stir evenly for 20 minutes, and irradiate it under ultraviolet-visible light. Next, place the stirred mixed solution on the photocatalytic reaction device, and after repeated stirring for several times, the photocatalytic degradation begins to have a chemical reaction, and the photocatalytic degradation solution is subjected to UV-vis spectrum test by an ultraviolet-visible spectrometer. According to the standard curve of methyl orange and the standard curve of p-chlorophenol, the UV-vis spectrum of methyl orange degradation solution and the UV-vis spectrum of p-chlorophenol (4-CP) degradation solution were tested to calculate the degradation rate, and the German Degussa product P-25 titanium dioxide was used as a comparative test sample.

#### 3.2.1 Photocatalysis experiment reaction device and light source emission spectrum

The schematic diagram of the photocatalytic experiment reaction device is shown in Figure 3.

Fix all the equipment in the photocatalysis experimental reaction device to ensure that the light does not deform, and use a fan to reduce heat treatment of the lamp source. Due to the long light time, the photocatalytic reaction temperature will gradually become higher, so use a cooling water jacket to avoid The temperature is too high.

The UV-visible light reflected by the metal halide lamp was used for the photocatalytic activity test. The light source emission spectrum is shown in Figure 4.

**Figure 3** Schematic diagram of photocatalytic experiment reaction device

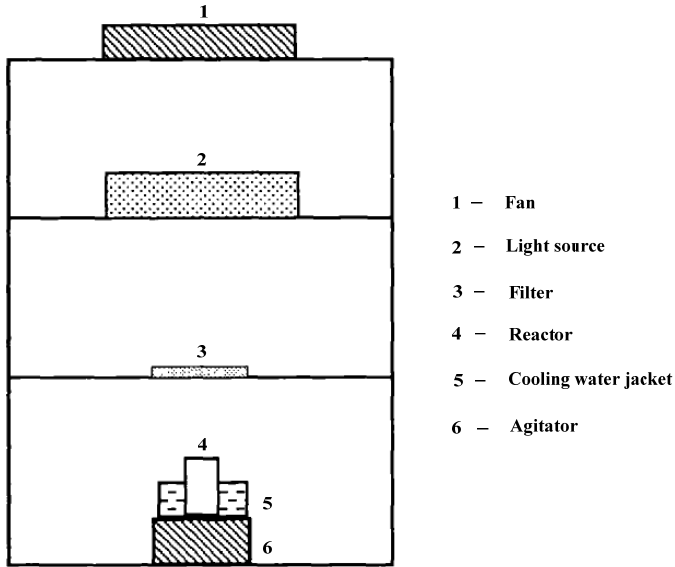
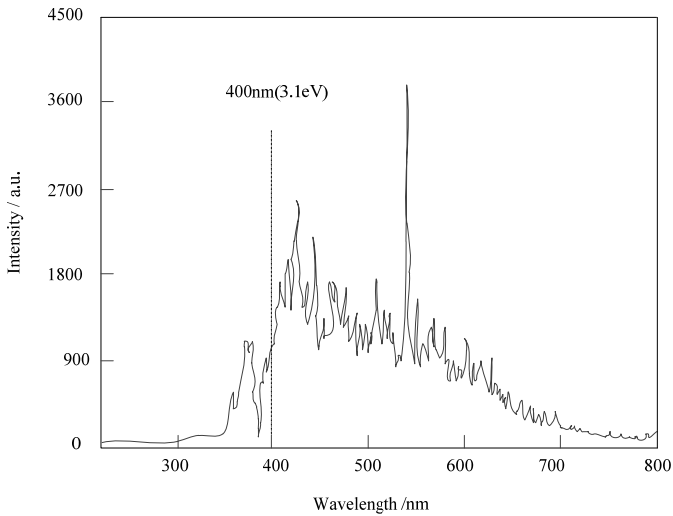


**Figure 4** Light source emission spectrum



It can be seen from the curve in Figure 4 that there are luminescence fluctuations at 350 nm, and there is a strong luminescence degree at 400 nm–550 nm, and the fluctuations are large. At 550 nm, the curve fluctuations are the largest.

### 3.2.2 Standard curve of methyl orange and *p*-chlorophenol

The photocatalytic activity of high-activity TiO<sub>2</sub> nanomaterials was degraded by methyl orange and para-gas phenol, and the photocatalytic activity of C-240 TiO<sub>2</sub> nanomaterials was characterised by light emission spectrum. According to the spectral characteristics of

the lamp source, obtain the standard curve of methyl orange and p-chlorophenol, and calculate the concentration of methyl orange and p-chlorophenol solution. The changes in absorbance of methyl orange and p-chlorophenol solution at different concentrations are shown in Figure 5 and Figure 6.

**Figure 5** The absorbance curve of methyl orange

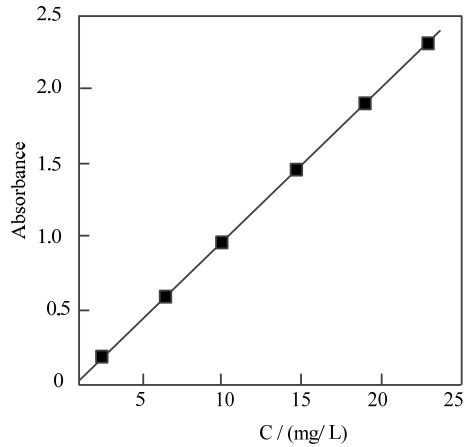
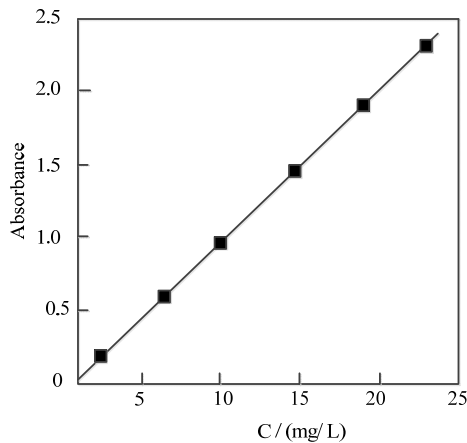


**Figure 6** Absorbance curve of p-chlorophenol



According to Figures 5 and 6, it can be seen that the curve changes in the two figures show a linear relationship. Fitting the absorbance curve at the methyl orange solution with the absorbance curve at the chlorophenol solution shows that the absorbance of the characteristic absorption peak varies with the concentration of  $C$ . Different, the calculation formula is as follows:

$$A_{(MO)} = 0.0027 + 0.076C \quad (3)$$

$$A_{(4-CP)} = 0.012 + 0.066C \quad (4)$$

In the formula,  $A_{(MO)}$  and  $A_{(4-CP)}$  respectively represent the peak absorbance.

Set the initial concentration of methyl orange or p-chlorophenol solution to 20 mg/L, then the corresponding degradation rate expression above is:

$$\eta_{(MO)} = 99.82 - 65.82A_{(MO)} \quad (5)$$

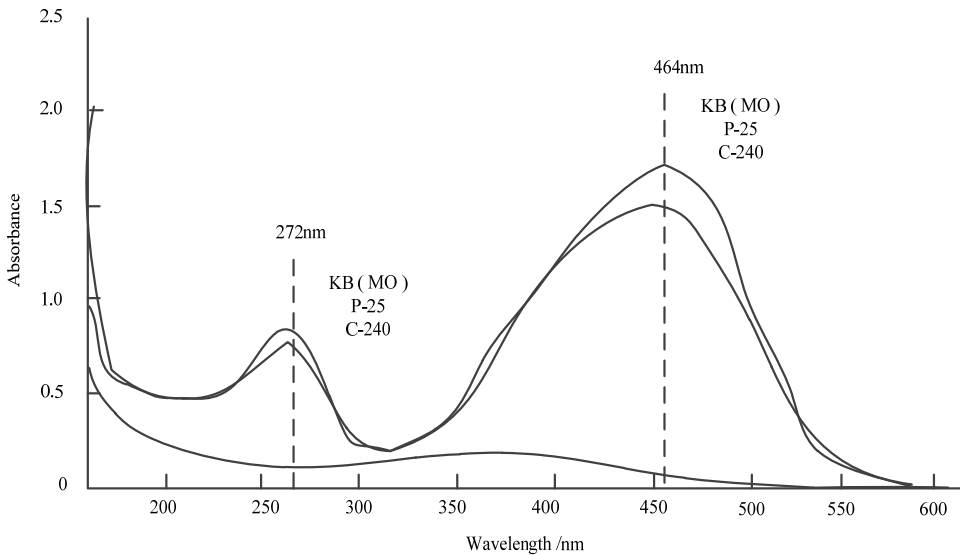
$$\eta_{(4-CP)} = 100.9 - 75.76A_{(4-CP)} \quad (6)$$

### 3.2.3 Characterisation of visible light catalytic activity of $TiO_2$ nanomaterials

#### 3.2.3.1 Visible light catalytic degradation of methyl orange

Taking KB (MO) as a blank sample of 20 mg/L methyl orange without adding  $TiO_2$ , after 60 minutes of visible light irradiation, the UV-vis spectrum of visible light catalytic degradation of methyl orange was obtained, as shown in Figure 7.

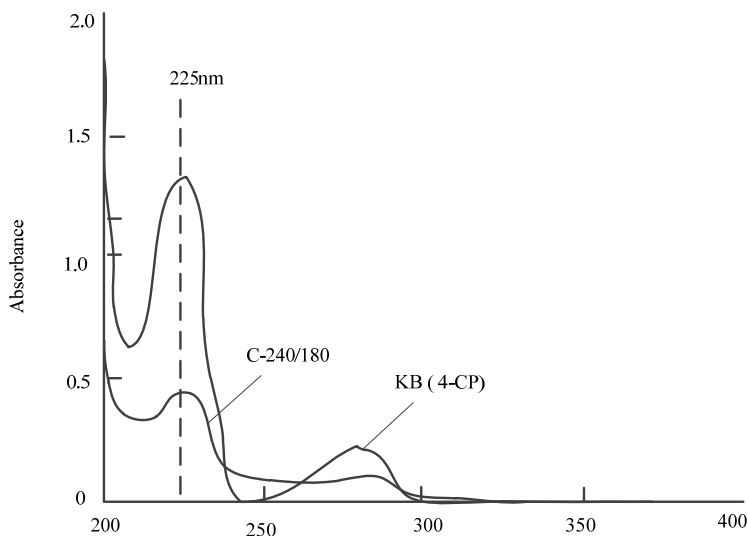
**Figure 7** UV-vis spectrum of methyl orange



Analysing the curve in Figure 7 shows that after 60 minutes, the peak absorbance of the visible light catalytic degradation of methyl orange is low. At 270 nm, the UV end absorption rate is low. According to the above standard curve, the degradation rate is calculated. Above 90%, while the calculated degradation rate of P-25 is only 10%, the degradation rate of methyl orange is higher than that of P-25.

#### 3.2.3.2 Visible light catalytic degradation of p-chlorophenol

The C-240 sample was pretreated, and the treatment time was one hour to obtain -240/180 sample. After 60 minutes of visible light, the UV-vis spectrum of visible light catalytic degradation of p-chlorophenol was obtained, as shown in Figure 8. Among them, KB (4-CP) is used as a blank sample of 20 mg/L p-chlorophenol without  $TiO_2$ .

**Figure 8** UV-vis spectrum of p-chlorophenol

Analysing the curve in Figure 8, the degradation rate of p-chlorophenol calculated according to the standard curve of p-chlorophenol absorbance is 66%, which shows that the C-240/180 sample can effectively photocatalyse the degradation of 4-CP. High degradation performance.

Acetone-pyridine-pyridine ternary mixed solvent is selected as the solvent, and C-240 TiO<sub>2</sub> nanomaterial sample is obtained according to the anodising method. The sample has a small crystal structure size and relatively uniform distribution, which is called single-phase anatase TiO<sub>2</sub> nanocrystalline. When the visible light band of the crystal is outside 450 nm, the visible light catalytic activity is better.

#### 4 Conclusions

In this paper, C-240 TiO<sub>2</sub> nanomaterial samples were prepared by anodising method. According to the X-ray diffraction method, the structure and composition of TiO<sub>2</sub> nanomaterials can be analysed and characterised. After X-ray irradiation, the wavelength of the rays has certain requirements, depending on the position of the diffraction peak and Different crystal materials can generate diffraction patterns of different sizes, which are closely related to the crystal structure. Compare and analyse the XRD pattern of the crystal structure with the XRD pattern generated by the experiment. The sample phase can be obtained from this, by electrochemical anodisation, obtain C-240 TiO<sub>2</sub> nanomaterial samples, study its performance based on transmission electron microscopy and high resolution transmission electron microscopy, select methyl orange and p-chlorophenol as highly active TiO<sub>2</sub> nanomaterials to degrade pollutants, and characterise and analyse them according to UV observe the absorption spectrum and observe the activity change. According to the U-VV is spectrum test of C-240 sample and commercial P-25 photocatalytic degradation of methyl orange for 60 minutes, it is known that the photocatalytic degradation of methyl orange by C-240 sample is greater than

90%, while the degradation rate of P-25 only 10%; after 60 minutes of photocatalytic degradation, observe the UV-vis spectrum of the C-240/180 sample, and it can be found that the degradation degree of the sample to 4-CP can reach 66%, which proves that the sample can be better 4-CP undergoes degradation treatment. Compared with P-25, 4-CP and methyl orange have higher visible light catalytic degradation. The high-activity photocatalytic nanomaterials prepared in this paper can degrade a large number of high-activity organic pollutants and lay the foundation for water pollution treatment.

## References

- Attallah, M.F., Youssef, M.A. and Imam, D.M. (2020) 'Preparation of novel nano composite materials from biomass waste and their sorptive characteristics for certain radionuclides', *Radiochimica Acta*, Vol. 108, No. 2, pp.137–149.
- Chen, J., Liu, Y. and Ye, Z. (2018) 'Preparation and catalytic performance of Fe<sup>3+</sup> doped nano-materials', *Characterization and Application of Nanoscience*, Vol. 11, No. 1, pp.1–11.
- Du, X., Wang, S., Du, Z., Xu, C. and Wang, H. (2018) 'Preparation and characterization of flame-retardant nanoencapsulated phase change materials with poly(methylmethacrylate) shells for thermal energy storage', *Journal of Materials Chemistry A*, Vol. 25, No. 18, pp.6–12.
- Hashempour, S. and Vakili, M.H. (2018) 'Preparation and characterisation of nano enhanced phase change material by adding carbon nano tubes to butyl stearate', *Journal of Experimental Nanoscience*, Vol. 13, No. 1, pp.188–198.
- Huang, L., Zhao, S. and Deng, Y. (2019) 'Preparation of rare earth Nd-doped ZnO nano-materials and its degradation of rhodamine B', *Inorganic Salt Industry*, Vol. 51, No. 8, pp.88–92.
- Ilieva, R., Dyulgerova, E., Petrov, O., Tarassov, M. and Vasileva, R. (2018) 'Preparation of hydroxyapatite/hyaluronan biomimetic nano-hybrid material for reconstruction of critical size bone defects', *Bulgarian Chemical Communications*, Vol. 50, No. 37, pp.97–105.
- Li, N., Zhao, Y., Cheng, C., Yang, Y., Yuan, H. and Carlini, H. (2018a) 'Preparation of core-shell magnetic nano-upconversion materials and its targeting effect', *Materials Letters*, Vol. 22, No. 15, pp.44–46.
- Li, Y., Song, Y., Tao, Y., Gao, F. and Tang, N. (2018b) 'Preparation of CdS/TiO<sub>2</sub> composite nano-net and study on its photocatalytic performance', *Imaging Science and Photochemistry*, Vol. 36, No. 3, pp.275–282.
- Liu, G., Jin, Y., Lu, Y., Hong, H. and Li, Z. (2019) 'Preparation of Ce<sup>4+</sup>-doped ZnO nanomaterials and its photocatalytic performance', *Journal of Nanjing Normal University (Engineering Technology Edition)*, Vol. 42, No. 3, pp.93–98.
- Mao, J., Li, W. and Zhang, X. (2019) 'Preparation of nano-materials for lithium/nano-ion battery anode and their energy storage performance in the field of transportation', *Journal of Nanoelectronics and Optoelectronics*, Vol. 14, No. 6, pp.801–811.
- Shankar, S., Oun, A.A. and Rhim, J.W. (2018) 'Preparation of antimicrobial hybrid nano-materials using regenerated cellulose and metallic nanoparticles', *International Journal of Biological Macromolecules*, Vol. 17, No. 5, pp.17–21.
- Shu, S., Wang, Y., Zhou, Y., Chen, S. and Jin, D. (2019) 'Preparation and performance of ZnO/g-C<sub>3</sub>N<sub>4</sub> micro-nano materials', *Chemical Research and Application*, Vol. 31, No. 8, pp.1505–1510.
- Wang, H. (2019) 'Preparation and application of functionalized micro-and nano-materials', *Shanxi Chemical Industry*, Vol. 39, No. 4, pp.11–13.
- Wang, L., Wan, J.Q., Wang, Y. and Wei, Y.C. (2020) 'The study on material preparation and adsorption properties of magnetic smaller sized Fe<sub>3</sub>O<sub>4</sub> load on multi-walled carbon nanotubes', *Key Engineering Materials*, Vol. 52, No. 23, pp.21–31.

- Wu, Z., Khan, M., Mao, S. and Lin, L. (2018a) 'Combination of nano-material enrichment and dead-end filtration for uniform and rapid sample preparation in matrix-assisted laser desorption/ionization mass spectrometry', *Talanta: The International Journal of Pure and Applied Analytical Chemistry*, Vol. 18, No. 9, pp.217–223.
- Wu, Z., Khan, M., Mao, S., Lin, L. and Lin, J. (2018b) 'Combination of nano-material enrichment and dead-end filtration for uniform and rapid sample preparation in matrix-assisted laser desorption/ionization mass spectrometry', *Talanta*, Vol. 27, No. 15, pp.217–223.
- Zeng, G., Zhao, L., Zeng, X. and Qiao, Z. (2018) 'Preparation progress of micro/nano-energetic materials', *IOP Conference*, Vol. 31, No. 9, pp.382–390.
- Zhang, S., Geng, Z., Zhang, W., Yang, X. and Li, Y. (2018) 'Preparation and luminescent properties of mesoporous (SBA-15)-Eu<sub>2</sub>O<sub>3</sub> nano materials', *Main Group Chemistry*, Vol. 17, No. 3, pp.197–209.
- Zheng, D-y., Li, M-y., Zhang, X-q. and Yue, J-q. (2019) 'Preparation of cellulose nanofibrils from rubber wood', *Packaging Engineering*, Vol. 40, No. 3, pp.100–107.
- Zhou, M., Jiang, S., Zhang, T., Shi, Y., Jin, X. and Duan, P. (2020) 'Construction and optoelectrical properties of chiral perovskite nanomaterials', *Progress in Chemistry*, Vol. 32, No. 4, pp.9–18.